Monitoring and Understanding VOC Induced Glass Corrosion Using Multi-modal Imaging Techniques

Deepshikha Sharma[1(✉)], Ulrike Rothenhaeusler[1], Katharina Schmidt-Ott[1], Marvin Nurit[2], Yuly Castro Cartagena[2], Gaetan Le-Goic[2], Edith Joseph[3,4], Sony George[5], and Tiziana Lombardo[1]

[1] Collection Centre, Swiss National Museum, Affoltern am Albis, Switzerland
Deepshikha.Sharma@nationalmuseum.ch
[2] Laboratoire Imagerie et Vision Artificielle, Université Bourgogne Franche-Comté, Dijon, France
[3] Haute Ecole Arc Conservation Restauration, University of Applied Sciences and Arts, HES-SO, Neuchâtel, Switzerland
[4] Laboratory of Technologies for Heritage Materials, University of Neuchâtel, Neuchâtel, Switzerland
[5] Norwegian University of Science and Technology, Gjovik, Norway

Abstract. Historical transparent glass is a fragile and challenging material. Deterioration of historical glass objects kept in presence of volatile organic compounds (VOCs) mainly formaldehyde, formic acid and acetic acid, is a known phenomenon. Similar issues were encountered with glass objects in the collection centre of the Swiss National Museum, belonging to 17th–20th century CE. Until 1999, these objects were stored in chipwood mobile shelving units (a source of VOCs) in conditions with fluctuating relative humidity (RH) levels and temperature. To study this phenomenon, model glasses were produced and subjected to accelerated aging with variable relative humidity and in the presence of acetic acid and formic acid. The aged samples were documented using digital techniques such as digital photography, reflectance transformation imaging, optical microscopy, and hyperspectral Imaging (HSI) to assess changes in their appearance and to detect early signs of corrosion. The results from the application of multi-modal imaging techniques to visualize the surface of transparent colourless glass show promise for the documentation of VOC induced corrosion phenomena on glass surfaces.

Keywords: Glass corrosion · Artificial aging · Optical microscopy · Digital photography · Reflectance transformation imaging · Hyperspectral imaging

1 Introduction

Historical-glass objects are very fragile and challenging for imaging techniques to acquire. Being colourless and transparent adds to the challenge. Given their historical

R. Furferi et al. (Eds.): Florence Heri-Tech 2022, LNME, pp. 359–375, 2023.
https://doi.org/10.1007/978-3-031-17594-7_27

and aesthetical value, such objects call for development of non-destructive investigation techniques for the assessment of glass corrosion phenomena.

Glass corrosion is a complicated process influenced by many different factors such as temperature, relative humidity, pollutants as well as composition of the glass itself. Several studies have been undertaken when it comes to outdoor atmospheric corrosion of glass [1–5]. However, the corrosion of glass kept in museum storage has not been studied at length and a few studies have focused on the corrosion of historical glass in indoor museum environments in the presence of Volatile Organic Compounds (VOCs) [6–12]. These studies used conventional analytical techniques such as Fourier transform infrared spectroscopy (FTIR), Raman spectroscopy, scanning electron microscopy coupled to energy dispersive spectroscopy (SEM-EDS), X-ray fluorescence, ion chromatography and secondary ion mass spectrometry. Nonetheless, the use of non-invasive and non-destructive techniques has not been reported extensively in the context of historical glass corrosion, which could provide faster and reliable monitoring and visualization of the various changes in appearance of altered glass. This work reports the preliminary results of the application of digital imaging techniques for the identification and monitoring of corrosion of transparent and colourless historical glass in the presence of VOCs, mainly acetic acid and formic acid.

1.1 Aims and Objectives

This project comes under the Cultural Heritage Analyses for New Generations (CHANGE) Marie Skladowska Curie Action-Integrated Training Network (MSCA-ITN CHANGE, change-itn.eu), and is hosted at the collection centre (SZ) of Swiss National Museum (SNM) in Affoltern am Albis. Various degradation phenomena were detected on some of the historical glass objects of the museum collections belonging to 17th–20th century. They were stored in mobile chipwood shelves for about 32 years from 1967 to 1999, without any temperature and relative humidity (RH) controls [13].

Chipwood is well known to emit VOCs, mainly formaldehyde, formic acid and acetic acid [6, 14, 15]. These compounds have been found to exacerbate the corrosion process in historical soda-lime silicate glasses kept in museums leading to the formation of formates and acetates on the surface [9, 10]. Previous assessments of the corroded historical glass objects of the SZ showed the presence of formates and acetates. Therefore, it was assumed that the long-term storage in chipwood mobile shelving units played an important part in their corrosion, even though they have been kept in improved storage conditions since 1999.

The main objective of this project under CHANGE is to establish a methodology and protocol based on multi-modal imaging techniques to identify VOC-induced glass corrosion in historical objects at an early stage without relying on clearly visible signs. It is also aimed to be able to monitor historical glass objects from time to time to detect any signs of corrosion or further degradation, thus leading to the exploration of imaging techniques, which can provide high-definition documentation of transparent glass objects.

2 Materials

To establish the required protocol for historical objects, the methodology is being developed first on model glasses, which are artificially corroded. These allow the study of early stages of corrosion. In addition, since they can also be analysed with destructive techniques, the data obtained with the imaging techniques can be correlated with those obtained with invasive investigations. The model glasses also do not pose any restrictions to traveling within the CHANGE consortium to foreign European institutes for analyses.

The model glasses were prepared by a traditional glass blower, according to a composition formulated by the Fraunhofer Institute for Silicate Research. They replicated the high-potassium alkali lime silicate composition (assessed by SEM-EDS on microsamples) of three corroded historical glass objects from the collections of the SNM. The composition of the historical objects was slightly modified and simplified to make the model glasses more susceptible to artificial aging within a short time frame. Using manufacturing techniques similar to the historical objects, the model glasses were first blown into cylinders and then sectioned into curved rectangular pieces of roughly 5 cm × 3 cm size and 1–2 mm thickness. They were then engraved with three lines each on the two long sides, to mimic the decoration of the historical objects and then labelled individually. Finally, their dimension and weight were documented.

The artificial aging of the model glasses was conducted in two borosilicate glass desiccators in ambient temperature of 20 °C–25 °C and relative humidity controlled using PROSorb® at 35% and 75%. The aging conditions for replicating the past storage conditions were VOC pollutants (acetic acid and formic acid) along with fluctuating humidity alternatively at 35% and 75% for equal number of days (PV). After every 3 months, one batch of eight model glass samples was withdrawn and characterised using multi-modal analyses up to a period of 12 months.

This paper will discuss the preliminary results from imaging techniques used for characterizing wet salt neocrystallizations (SNs) and microcracks developed as a result of glass corrosion on transparent model glasses. Wet SNs are deliquescent salts formed due to the interaction of VOCs with the alkali cations leached from the glass during corrosion.

3 Experimental Methods

The experimental methods are described in the following section in the order of macro- (i.e., digital photography and reflectance transformation imaging (RTI)) to micro-imaging (i.e. optical microscopy), of the model glasses, up to molecular level information with hyperspectral imaging (HSI), which provides both spatial and spectral information.

3.1 Digital Photography

Three different setups were used for photography of the samples using transmitted light (TL), transmitted and cross-polarized light (TCPL) and reflected light (RL). Additionally, TCPL photography should provide visualization of mechanical strains developed as colourful anisotropic patterns on corroded glass. It is well-known that colourful

anisotropic patterns (equivalent of birefringence for minerals) develop when glass is badly annealed, or subjected to compression, bending or stretching. This can be understood using the photoelasticity theory [16]. Our hypothesis is that strain-producing inhomogeneities might be developed because of weathering and corrosion as well.

All the model glasses were photographed before artificial aging and after each withdrawal, so that the changes in visual appearance can be detected by comparing the pictures taken before and after aging. Every batch of eight model glasses was photographed together and in sets of two, at different exposures of shutter speed with fixed aperture, on manual mode using a digital camera with white LED light source.

The photography setup consists of a Nikon D800 Digital Single-Lens Reflex (DSLR) camera fitted on a camera stand with a light table (60 × 60 cm) at the bottom of the stand kept in a dark room with windows covered by thick black paper to avoid any stray lights. The lens used was a Nikon aspherical micro lens of 60 mm focal length.

For TL photography, the glasses were placed on printed and labelled grids on acetate sheets, which were cut to create windows to ensure consistent positioning of the glass samples and clearly visible labels. This acetate sheet was placed on the light table at the highest light intensity of approx. 4000 lx, which was measured with a luxmeter and was found to be homogenous. The photography was done at manual mode with aperture F16, ISO 100 and four different shutter speeds at 1/20, 1/30, 1/50 and 1/80 of a second.

For TCPL photography (Fig. 1), the same setup was used with a Hama circular polarization filter fitted on the camera lens along with a ROSCO linear polarization sheet with the labelled acetate sheet placed on top of it. Once the glasses were set in their right place, the polarization filter on the camera was rotated to find the darkest background under the glass samples (which is the angle of total extinction) and then photos were taken at manual mode with aperture of F16, ISO 100 with five different shutter speeds at 1/1.3, 1/1.6, 1, 1.3 and 2 s.

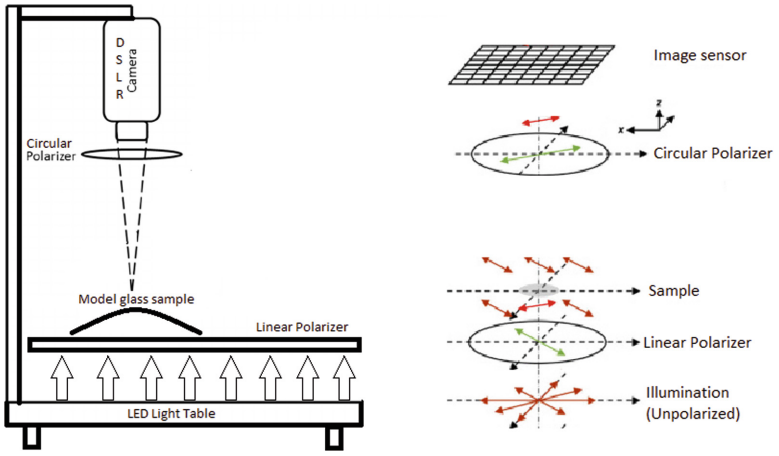

Fig. 1. Schematic diagram of the TCPL photography setup showing incident light directions with red arrows and polarizing direction with green arrows.

For RL photography, light from two standing studio lights (diffused white LED lights) kept on either side of the sample were used and the samples were placed on a black cardboard background. Photos were captured at aperture F16, ISO 100 and shutter speeds at 1/1.3, 1/1.6, 1, 1.3 and 1.6 s, in manual mode.

3.2 Reflectance Transformation Imaging

RL on glass surfaces can also be studied through Reflectance Transformation Imaging (RTI). RTI combines many photographs of the same artefact taken from a camera on a fixed position, while varying the light position at each picture. Different methods are used to process RTI data such as the polynomial texture mapping (PTM), hemispherical harmonics (HSH) and discrete modal decomposition (DMD) [17] (Castro et al., 2020). The most popular method to process RTI data is PTM, which was initially developed by Tom Malzbender [18]. One of the most known features allowed by the RTI data, is the creation of a relightable file, which allows an interactive visualisation of the imaged object under different lighting positions. RTI acquisition of transparent surfaces are complicated due to the various possible interactions between the surface and its light environment [19]. Although, there have been some previous works on relighting visualizations of glass objects [20, 21].

Besides the relighting, RTI data can be used to produce normal maps using local geometry as well as statistical maps using local reflectance [22]. Both maps are generated using descriptors which can characterise different local reflectance features and in turn different degradation phenomena on corroded glass surfaces. This is possible because light is reflected differently from isotropic or anisotropic features on the surface. Reflectance response of an isotropic geometry is homogenous and does not vary with the angle of incident light, while for an anisotropic geometry, it varies depending on whether the angle of incident light is parallel (low response) or perpendicular (high response), so the scale of variation is large. In this case, RTI data were processed using Matlab, to generate maps of geometrical descriptors (Dx and Dy) and statistical descriptors (median and kurtosis).

- Dx and Dy are used to define a 3D surface, projected on the x-y plane. Dx and Dy are local geometric descriptors that allow to highlight anisotropic appearance characteristics measured along x and y axis, respectively. Moreover, descriptor Dy describes the change in reflectance per pixel distribution along y axis and Dx describes change along x axis (Fig. 2a). In other words, Dx and Dy give information about features of surface alteration and their directionality, Dx showing changes from left to right and Dy showing changes from top to bottom.
- The median divides the pixel distribution into two parts, so that 50% of the distribution is below the median and 50% above (Fig. 2b). It is often used instead of the mean when the distribution has outliers. The use of median is to understand whether a point on the surface has a constant or exceptional behaviour.
- Kurtosis allows to describe the tails of the reflectance per pixel distribution or 31.8% of the values (Fig. 2b) and thus to estimate the presence or absence of outliers. The further the value is from the mean or median, the more it contributes to the kurtosis, so a high kurtosis value indicates the presence of outliers in large or small quantities.

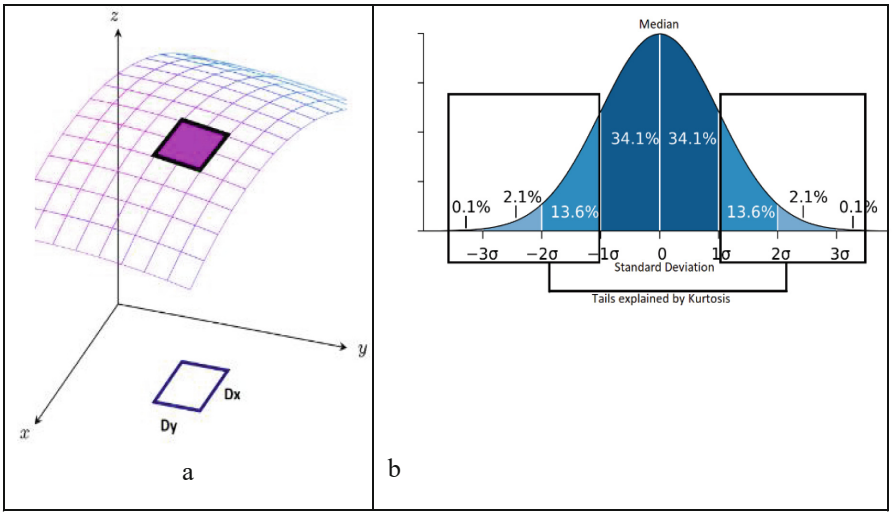

Fig. 2. a) Diagram showing local descriptors Dx and Dy on the 3D sample surface b) A normal distribution curve explaining median and kurtosis descriptors.

The RTI datasets presented in this paper were acquired using a custom designed dome-based system [22]. This is a completely automated system, with a single light source held on a motorized arc that allows the light source to be placed at any desired position of the angular space defined between 0° to 360° for azimuth (Ø) and 0° to 75° for elevation of the dome (ϴ) with a radius of 220 mm. The system is equipped with a 12.4-megapixel monochrome camera, which along with a motorized zoom and focus forms an optical system that offers high quality images. A white LED light was used as the light source designed to be integrated into the acquisition system. Thanks to the synergy between motorized hardware and custom-made control software, this robust system ensures highly accurate and repeatable RTI acquisitions [22].

3.3 Optical Microscopy

Due to light reflection, glass can be difficult to study under an optical microscope. A universal microscope was used in different configurations such as TL, RL, TCPL and dark field imaging, to visualize glass corrosion features. Optical microscopy was performed using a Zeiss AxioLab Universal microscope in reflectance and transmission mode, employing both non-polarized and cross-polarized light. This apparatus was exclusively used to examine smaller samples that fit on the stage, and photos were captured at 1.25x–25x magnification using an Axiocam 305 colour camera and Zeiss blue software. In an attempt for quantification of the corrosion progression, the images were processed using open-source Fiji distribution of ImageJ software [23] to quantify the size and area of the deliquescent SNs automatically using threshold adjustment of the dark SNs against brighter background. Usually, an area with good contrast between the SNs and the background surface is chosen for the algorithm to work. SNs can then be automatically measured for size and numbers using ‘Analyse particles’ plugin. The quantification was

performed over a fixed area of 1700 × 1400 μm^2 for each microphotograph taken at 2.5x magnification.

3.4 Hyperspectral Imaging

Hyperspectral imaging (HSI) has grown in popularity as a non-invasive approach for examining works of art [24] and references therein. This approach allows for the acquisition of spectral information across a large region of interest, enabling for the identification, mapping and visualisation of the artefact's component materials. Few applications of this method to stained glass have been published [25–27]. However, there has been no application yet on characterization of glass corrosion using HSI.

The Hyperspectral image acquisition was carried out using two imaging systems: one covering the visible and near infrared region (VNIR, 400–1000 nm) and another one in the short-wave infrared region (SWIR, 1000–2500 nm). The cameras used are HySpex VNIR-1800 and a SWIR-384 push-broom system developed by Norsk Electro Optikk As. The VNIR camera acquires 186 images in the visible and near-infrared (VNIR) range, with a spectral sampling of 3.26 nm and a resolution of 1800 pixels across the track. The SWIR camera acquires 288 images in the SWIR range, with a spectral sampling of 5.45 nm and a resolution of 384 pixels across the track. Two cameras were set at a fixed focus distance of 30 cm from the model glass samples. Trials were performed with different light sources and their geometric positions, imaging parameters and reflected and transmitted light to identify the best configuration for the acquisition of the corroded and reference model glass samples. The HSI data was collected in transmittance mode. Halogen lamps were used as the light sources and are placed below the moving translation stage in a way that light will transmit through a glass diffuser and the glass sample to be studied. Acquisition parameters such as integration time, frame averaging etc. are set so that enough light reaches the camera and are synchronized with the speed of the moving stage. The raw data from both the cameras was corrected to radiance and processed using ImageJ to generate the HSI transmittance data cubes.

4 Results

4.1 Digital Photography

As can be seen with the digital photographs, the white background doesn't provide a very clear image of the model glasses and the exposure time (shutter speed) should be reduced to be able to capture details such as engravings for the transparent glass objects. Additionally, SNs, microcracks, dust particles and bubbles are not discernible with transmitted light photography (Fig. 3).

Photos acquired in TCPL photography show that no global strain has developed until 12 months of aging for any of the model glass samples. Nonetheless, the use of TCPL shows a real improvement compared with TL, as the resulting black background shows clearly discernible dust particles on the glass surface and bubbles (Fig. 4a). In certain cases, some SN are also visible. In the present example, they can be noticed at the top of the samples (Fig. 4b).

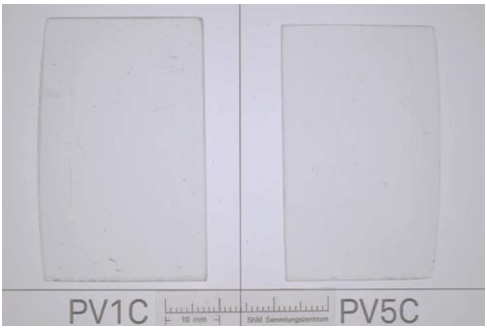

Fig. 3. Photographs of PV model glasses aged for 9 months, acquired in TL

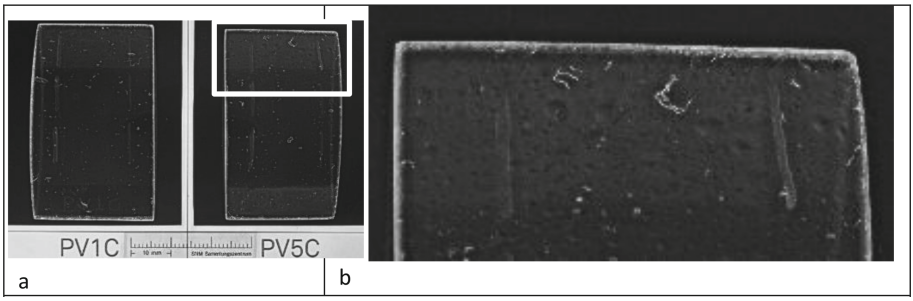

Fig. 4. Photographs of PV model glasses aged for 9 months, acquired in a) TCPL mode and b) enlarged section

Photographs acquired in RL clearly show the presence of deliquescent SNs in specific regions of the samples only at incident light angles suitable to capture specular reflection from the SNs (Fig. 5a). However instead of clearly visualizing the shape of the SNs (i.e. drops), only specific specular reflections can be seen (Fig. 5b).

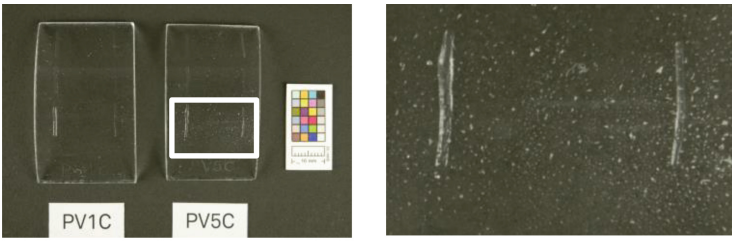

Fig. 5. RL photographs of PV model glasses a) aged for 9 months, with a white rectangle highlighting specular reflection from the SN, and b) enlarged rectangular area showing SN.

4.2 Reflectance Transformation Imaging

RTI maps were generated for a specific region in the centre of every model glass. Here all the maps correspond to an area acquired from a model glass aged to 9 months (Fig. 6a). Figure 6b shows one of the images acquired by RTI which helps to interpret the maps discussed in this section (Figs. 7, 8 and 9).

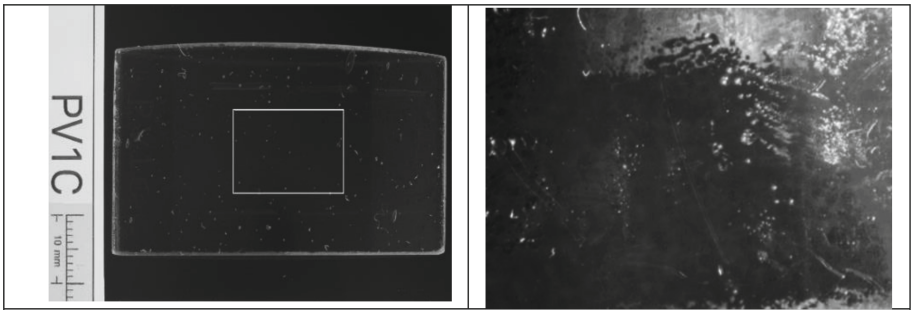

Fig. 6. a) TCPL photograph of PV model glass aged for 9 months, with a white rectangle highlighting the area acquired by RTI (16 × 12 mm^2), b) White light image (16 × 12 mm^2) from RTI setup.

The Dx map (Fig. 7a) shows a few circular features which are SNs along with a few elliptical features i.e. bubbles, and irregularly shaped dust particles, while the Dy map (Fig. 7b) shows a larger number of SNs and bubbles along with some cracks (inside white rectangles) and dust particles.

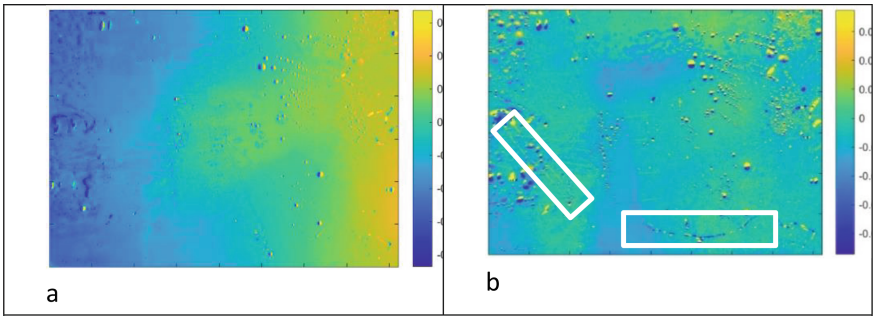

Fig. 7. a) Dx map of PV model glass aged for 9 months showing SN and dust particles, b) Dy map of PV model glass aged for 9 months showing SN, microcracks (inside white rectangles) and dust particles.

RTI images were taken from 200 different light positions homogenously distributed around the dome. Irregularly shaped features such as the dust particles and circular or elliptical features i.e. the bubbles, can be seen at more than 100 light positions since they have high values in the median map while the cracks and deliquescent SNs are only

visible in less than 100 light positions and therefore cannot be seen in the median map (Fig. 8a). In other words, only the non-transparent or reflective features on the glass surface can be seen in the median map.

The further the value is from the mean or median, the more it contributes to the kurtosis, so a high kurtosis value indicates the presence of outliers in large or small quantities. In the case here, bubbles and dust particles have lowest kurtosis values since they fall in the range close to the median, while the micro-cracks and SNs have higher kurtosis showing that they fall within the tails of the pixel distribution (Fig. 8b). In other words, micro-cracks and SNs are the outliers of the pixel distribution.

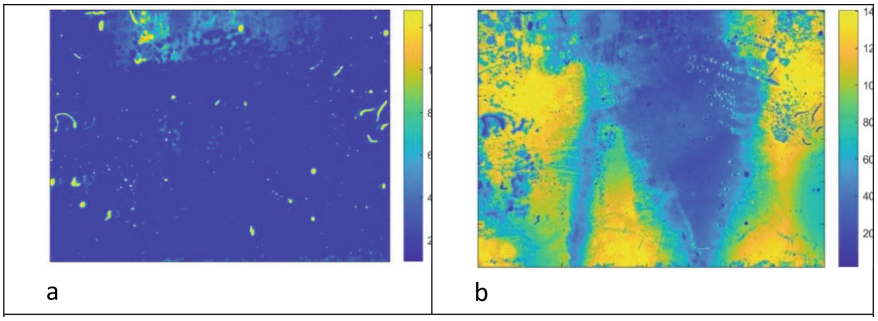

Fig. 8. a) Median map of PV model glass aged for 9 months showing bubbles in the glass and dust on the surface, b) Kurtosis map of PV model glass aged for 9 months showing SNs, dust, microcracks and scratches.

4.3 Optical Microscopy

SNs

SNs can be clearly seen in the images as circular or elliptical features. The preliminary results show clearly that RL allows to visualize the SNs of all sizes on the glass surface better than TL (notice the areas within the white rectangles in Fig. 9. Dark field microscopy also clearly shows SNs (Fig. 10).

The SNs were measured for size and numbers using bright field RL microphotographs (Figs. 11 and 12) since the dark field images lack contrast between the SNs and the background surface. Table 1 shows the correlation between the number and size of SNs, percentage area covered by SNs (total SN area/total surface area) and the aging time for the PV model glasses withdrawn at 3, 6, 9 and 12 months. As can be seen from, the percentage area covered increased by only 3.08% between 3 and 6 months after which it decreased considerably at 9 months as compared to 3 months (58% reduced) and decreased until 12 months, with similar values at 9 and 12 months.

Despite the large standard deviation due to a high variability in the SN sizes, a tendency towards increase in the size can be seen between 3 and 6 months with reduction in the number of SNs indicating coalescence of the SNs. The average size of SNs shows a tendency of decrease from 9 months onwards along with increasing number of SNs. This

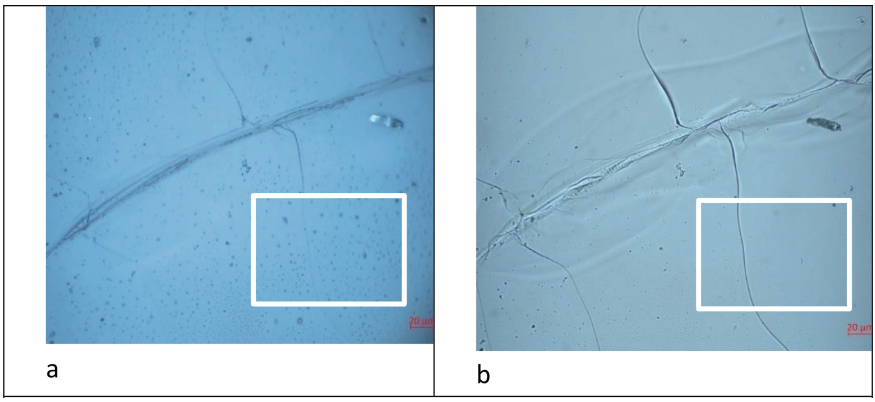

Fig. 9. Microphotographs at 25x original magnification showing microcracks and small SNs on the PV model glass surface aged for 3 months using a) RL or b) TL mode, with white rectangle highlighting SNs.

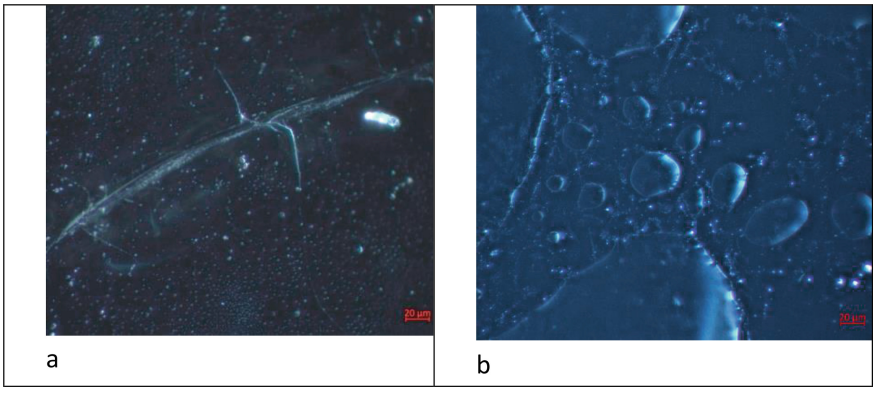

Fig. 10. Dark field microphotographs of PV model glass aged for 3 months, at 25x original magnification, showing a) cracks and small SNs, and b) large SNs.

trend shows that after reaching a certain dimension, the large sized SNs start running down the glass surface while newer and smaller SNs continue forming (Table 1). Since the approach at measuring SNs is proved to be successful, it will be applied to further model glass samples to obtain statistically representative results which will then be used to understand corrosion mechanisms.

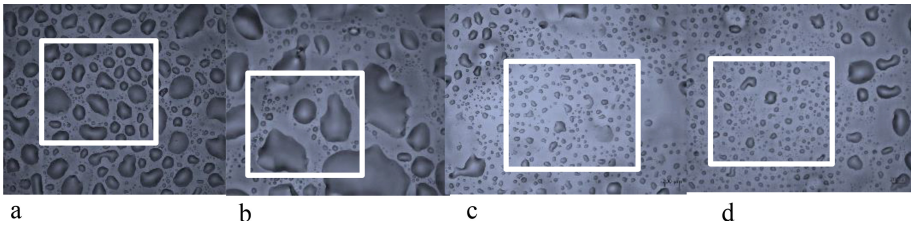

Fig. 11. RL microscopic images at 2.5x original magnification of PV model glasses aged for a) 3 months b) 6 months c) 9 months d) 12 months, showing area selected for SN quantification

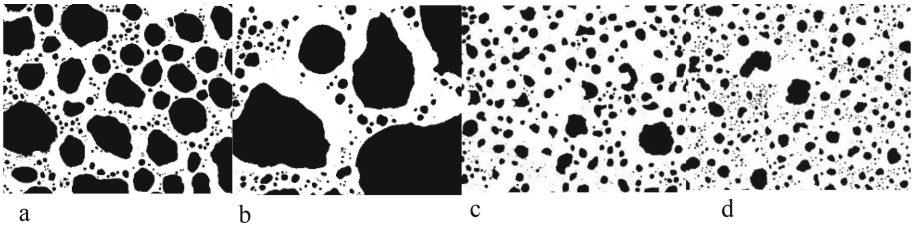

Fig. 12. Threshold adjusted images of the highlighted areas to perform digital particle analyses for measuring SN size and coverage area in an area of 1700 × 1400 μ^2 (white rectangle area indicated on Fig. 11), for PV glasses aged for a) 3 months b) 6 months c) 9 months d) 12 months.

Table 1. Table showing number, size of SNs and percentage area covered for different duration of aging for the PV model glass

	3 months	6 months	9 months	12 months
Number of SNs	504	232	468	888
Average SN size (μm^2)	2533.5 ± 10579.32	5819.76 ± 37949.07	1220.04 ± 3198.28	630.27 ± 1950.78
Percentage area covered	53.65	56.73	23.99	23.52

Microcracks

For the visualization of microcracks, different microscopy modes were used: RL in bright and dark field, TL, and TCPL. Microcracks are easily visible using TL and RL modes in bright field (Fig. 9). It can be clearly seen that TL (Fig. 9b) gives more details of the cracks than RL (Fig. 9a). Dark field microscopy can also show larger microcracks with better contrast (Fig. 10a).

Cross-polarization microscopy shows colourful anisotropic patterns inside the crack as shown in Fig. 13. These patterns can only be seen at 25x magnification and higher and are very likely evidence of the formation of strains due to corrosion in the model glass. Hence, it can be clearly seen that although the alteration-induced strains are not intense

and widely distributed in the glass to be detected by macro-level TCPL photography (Fig. 4a), they are present at microscale as early as after 3 months of aging.

Apart from this, it is interesting to note a sub-surface feature surrounding the region of the crack in both TL bright field (Fig. 9b) and TCPL microphotographs (Fig. 13). This feature can possibly be studied based on fracture analysis technique described by Davison [28] but further understanding and information is required for a definite interpretation.

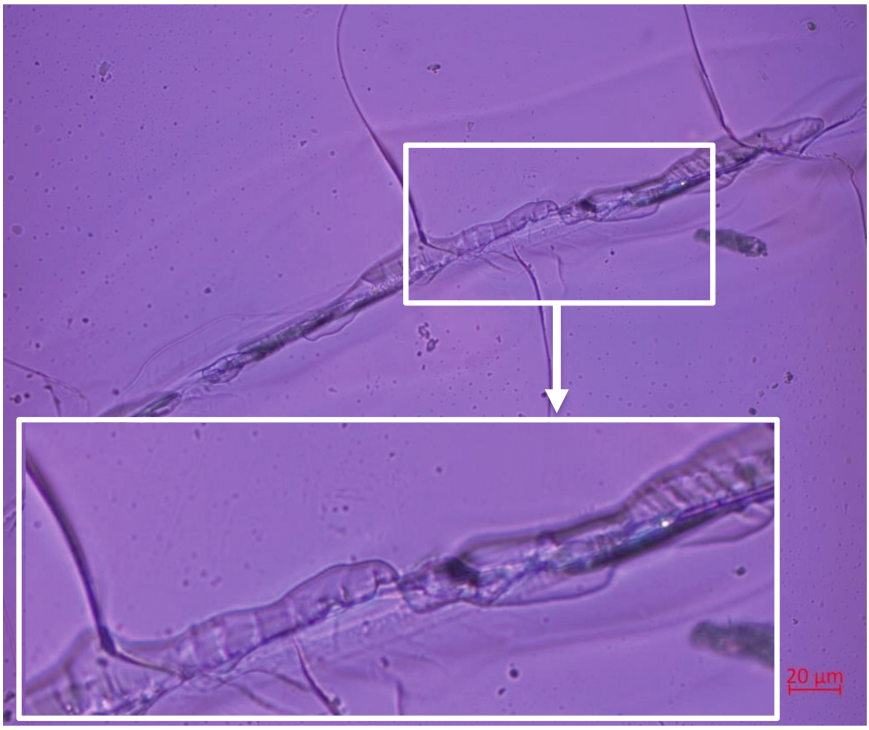

Fig. 13. TCPL microphotograph with lambda filter, at 25x original magnification, showing colourful anisotropic patterns inside the crack on the PV model glass surface aged for 3 months (Inset: enlarged section of the crack).

4.4 Hyperspectral Imaging

The VNIR images has higher spatial resolution but does not show any micro-cracks, SN or dust particles present on the surface of the corroded glass sample. Only the engravings and bubbles are clearly visible (Fig. 14a). On the other hand, the SWIR image with much lower spatial resolution shows SN on the glass surface. Indeed, dark circular features are observed in Fig. 14b and corresponding to spectral bands at 1415 nm and 1905 nm, which are known to be combination or overtone vibrational bands of water interacting with the silicate matrix [29].

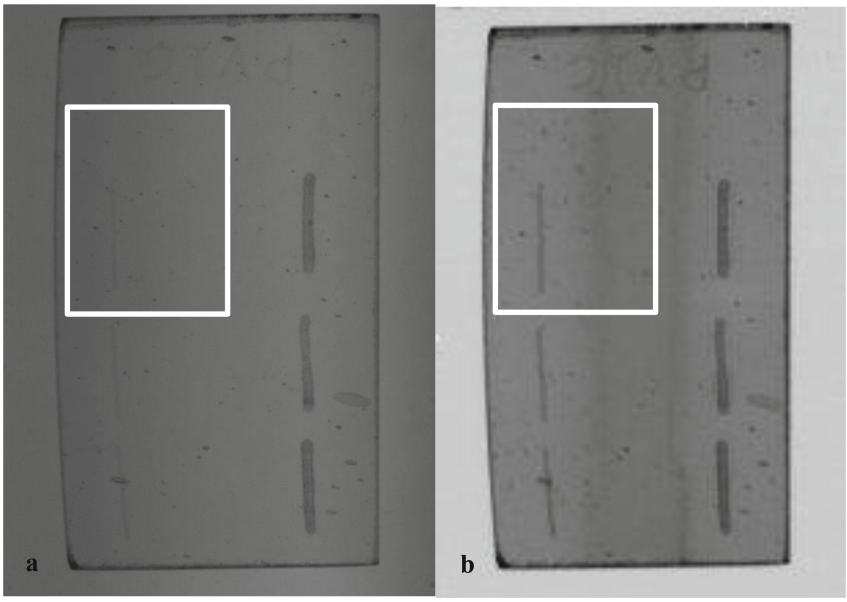

Fig. 14. Hyperspectral images of PV model glass aged for 9 months using an a) Image from VNIR camera at 998.1 nm and b) Image from SWIR camera at 2516.6 nm, with white rectangle highlighting SNs.

5 Discussion

The results presented in this paper are aimed at describing four non-invasive techniques provided information about the corroded model glass surfaces from macro level to molecular level. Results show that these techniques are useful to characterize VOC-induced glass corrosion, expressed in terms of SN and microcracks. While some of these are conventional imaging techniques, some other advanced ones are at an early immature stage for visualizing glass corrosion and need further development.

TL photography is commonly used for artistic photography of glass objects for commercial purposes but is not effective here to visualize the surface degradation features on corroded glass. TCPL photography is used by industries to assess the quality of glass and presence of strains in the glass. The TCPL photographs of the samples show features such as bubbles and dust particles on the surface of the transparent glass very clearly due to the black background. However, due to the lack of development of strains at macroscale, no colourful anisotropic patterns could be visualized. Nonetheless, TCPL photography offers a much better standardised photographic documentation setup for transparent glass, as performed on a black background rather than TL photography using plain white background. It is an inexpensive and easy to arrange setup for photographing glass. The RL photography with a black cardboard background can also show SN along with bubbles and dust particles but only at specific areas and light positions. Therefore, the information gained is not standardised and reproducible with the setup used. This issue was overcome by using a standardised setup such as for RTI.

RTI is a technique, which can provide standardised and reliable data using reflected light. This technique is useful for creating relighting visualizations for transparent glass and shows micro-cracks along with SN, bubbles and dust particles, even when they are not easily discernible with digital photography. The exploratory results from the RTI data using local reflectance and geometric descriptors are promising in visualizing degradation phenomena and surface features using specific statistical parameters. The system used can provide scientific data and it is still under development. Post processing of the data to generate the maps can be time-consuming and requires a powerful computer and a specific RTI acquisition user interface. Therefore, at this stage, its implementation using mathematical descriptors as a documentation tool, show promise but needs more development.

Optical microscopy is a useful technique for visualizing glass corrosion and is easily available in most laboratories and museums. Using different modes with transmitted light, reflected light in bright and dark field and TCPL, better visualization can be gathered. The images can be further processed to quantify degradation features for characterizing glass corrosion. Nevertheless, optical microscopy poses restrictions to the size of the objects and the regions that can be examined, due to the limitations of the stage size and working distance. While smaller glass objects and flat surfaces can be easily investigated, large glass objects and curved interior surfaces pose problems.

Hyperspectral imaging with VNIR camera did not provide any further information on the degradation phenomena but provides a better visualization than transmitted light photographs clearly showing the engravings and bubbles. The SWIR data are promising and can provide information on the hydration of the glass matrix using a spectral range of 1000–2500 nm, which otherwise is only accessible through fibre optic reflectance spectroscopy. Although the HSI setup is expensive, it provides very fast data acquisition, has practically no size limitations and requires easily learnable post processing. However, the volume of data generated is quite important and would require considerable space in storage device.

6 Conclusion

This paper discusses the preliminary results on the application of four multi-modal techniques to visualize surface degradation phenomena, especially SN and micro-cracks, on transparent colourless glass artificially corroded in the presence of VOCs and fluctuating humidity. Although microscopy and digital photography are part of standard documentation techniques for glass, this paper proves that it is possible to use further image processing to enhance and quantify the obtained information for the identification of glass corrosion and its extent on model glasses with composition like historical glass objects. Many of these degradation phenomena cannot be seen or documented with naked eyes or with digital photography. Therefore, advanced techniques like RTI and HSI need further development and processing to give quantifiable data for the characterization and visualization of early stages of historical glass corrosion. The exploratory phase results are encouraging to advance towards further data acquisition and analyses to correlate these results and generate non-invasive identification and monitoring protocols for VOC-induced corrosion in transparent historical glasses. Finally, the transferability

of the results obtained on the model glass to larger 3D objects will be explored when the investigation of real museum objects with 3D shapes (e.g., flasks, bottles, cups etc.) will be performed.

Acknowledgements. This research was carried out as part of the CHANGE (Cultural Heritage Analysis for New Generation) Innovative Training Network project funded by the European Union's Horizon 2020 research and innovation programme under the Marie Skłodowska-Curie grant agreement No. 813789. The authors express their gratitude to the colleagues at Swiss National Museum, Affoltern am Albis, Switzerland, Norwegian University of Science and Technology, Gjovik, Norway and Université Bourgogne Franche-Comté, Dijon, France, for their help and support. In addition to this, we would like to express our gratitude towards Katrin Wittstadt of Fraunhofer Institute for Silicate Research (ISC), Bronnbach, Germany, for formulating the composition of the model glasses and towards traditional glass blower Alain Guillot, Le Bourg, Boisse, France, for manufacturing them.

References

1. Alloteau, F., Majérus, O., Biron, I., Lehuédé, P., Caurant, D., Seyeux, A.: Temperature-dependent mechanisms of the atmospheric alteration of a mixed-alkali lime silicate glass. Corros. Sci. **159**, 108129 (2019)
2. Gentaz, L., Lombardo, T., Chabas, A., Loisel, C., Neff, D., Verney-Carron, A.: Role of secondary phases in the scaling of stained-glass windows exposed to rain. Corros. Sci. **109**, 206–216 (2016)
3. Hellmann, R., et al.: Nanometre-scale evidence for interfacial dissolution-reprecipitation control of silicate glass corrosion. Nat. Mater. **14**(3), 307–311 (2015)
4. Lenting, C., Plümper, O., Kilburn, M., Guagliardo, P., Klinkenberg, M., Geisler, T.: Towards a unifying mechanistic model for silicate glass corrosion. NPJ Mater. Degrad. **2**(1) (2018)
5. Majérus, O., Lehuédé, P., Biron, I., Alloteau, F., Narayanasamy, S., Caurant, D.: Glass alteration in atmospheric conditions: crossing perspectives from cultural heritage, glass industry, and nuclear waste management. NPJ Mater. Degrad. **4**(1), 1–16 (2020)
6. Greiner-Wronowa, E.: Influence of organic pollutants on deterioration of antique glass structure. Acta Physica Polonia A **120**(4) (2011)
7. Robinet, L., Eremin, K., Coupry, C., Hall, C., Lacome, N.: Effect of organic acid vapors on the alteration of soda silicate glass. J. Non-Cryst. Solids **353**(16–17), 1546–1559 (2007)
8. Robinet, L., Fearn, S., Eremin, K.: Understanding glass deterioration in museum collections: a multi-disciplinary approach. In: 14th Triennial Meeting the Hague Preprints, pp. 139–145 (2005)
9. Robinet, L., Hall, C., Eremin, K., Fearn, S., Tate, J.: Alteration of soda silicate glasses by organic pollutants in museums: mechanisms and kinetics. J. Non-Cryst. Solids **355**(28–30), 1479–1488 (2009)
10. Verhaar, G., van Bommel, M.R., Tennent, N.H.: Weeping Glass: The Identification of Ionic Species on the Surface of Vessel Glass Using Ion Chromatography (2016)
11. Verhaar, G.: Glass sickness: detection and prevention: investigating unstable glass inmuseum collections (2018)
12. Rodrigues, A., Fearn, S., Palomar, T., Vilarigues, M.: Early stages of surface alteration of soda-rich-silicate glasses in the museum environment. Corros. Sci. **143**, 362–375 (2018)
13. Schwarz, A.: "Kranke" Gläser : Formaldehydemission und Glaskorrosion : Untersuchungen am Beispiel der Glassammlung des Schweizerischen Landesmuseums. Zeitschrift Für Schweizerische Archäologie Und Kunstgeschichte **59**, 371–384 (2002)

14. Odylha, M., Bergsten, C.J., Thickett, D.: Volatile organic compounds (VOCs) released by wood. In Basic Environmental Mechanisms Affecting Cultural Heritage. Understanding Deterioration Mechanisms for Conservation Purposes. In: COST Action D, vol. 42, pp. 107–133 (2010)
15. Schieweck, A., Delius, W., Siwinski, N., Vogtenrath, W., Genning, C., Salthammer, T.: Occurrence of organic and inorganic biocides in the museum environment. Atmos. Environ. **41**(15), 3266–3275 (2007)
16. Illguth, M., Schuler, C., Bucak, Ö.: The effect of optical anisotropies on building glass façades and its measurement methods. Front. Archit. Res. **4**(2), 119–126 (2015)
17. Castro, Y., et al.: Calibration of spatial distribution of light sources in reflectance transformation imaging based on adaptive local density estimation. J. Electron. Imaging **29**(04), 041004 (2020)
18. Malzbender, T., Gelb, D., Wolters, H.: Polynomial texture maps. In: Proceedings of the 28th Annual Conference on Computer Graphics and Interactive Techniques, pp. 519–528 (2001)
19. Kitanovski, V., Hardeberg, J.Y.: Objective evaluation of relighting models on translucent materials from multispectral RTI images (2021)
20. Dittus, A.M.: Reflectance Transformation Imaging (RTI) Eine Methode zur Visualisierung struktureller Oberflächenmerkmale. Restauro **4**, 24–31 (2015)
21. Mytum, H., Peterson, J.R.: The application of reflectance transformation imaging (RTI) in historical archaeology. Hist. Archaeol. **52**(2), 489–503 (2018). https://doi.org/10.1007/s41636-018-0107-x
22. Nurit, M., le Goic, G., Chatoux, H., Maniglier, S., Jochum, P., Mansouri, A.: RTI derived features maps and their application for the assessment of manufactured surfaces. Comput. Vis. Image Underst. (2021)
23. Schindelin, J., et al.: Fiji: an open-source platform for biological-image analysis. Nat. Methods **9**(7), 676–682 (2012)
24. George, S., et al.: A study of spectral imaging acquisition and processing for cultural heritage. In: Digital Techniques for Documenting and Preserving Cultural Heritage, pp. 141–158 (2018)
25. Palomar, T., Grazia, C., Cardos, I.P., Vilarigues, M., Miliani, C., Romani, A.: Analysis of chromophores in stained-glass windows using visible hyperspectral imaging in-situ. Spectrochim Acta A Mol Biomol Spectrosc **223**, 117378 (2019)
26. Cortelazzo, G.M., Poletto, L., Bertoncello, R.: New trends in imaging spectroscopy: the non-invasive study of the Scrovegni Chapel stained glass windows. In: Proceedings SPIE, vol. 8084 (2011)
27. Babini, A., George, S., Hardeberg, J.Y.: Hyperspectral imaging workflow for the acquisition and analysis of stained-glass panels (2021)
28. Davison, S.: Conservation and Restoration of Glass (2006)
29. Zaleski, S., et al.: Application of fiber optic reflectance spectroscopy for the detection of historical glass deterioration. J. Am. Ceram. Soc. **103**(1), 158–166 (2020)